

Probing Lorentz and CPT Violation in a Magnetized Iron Detector using Atmospheric Neutrinos

Animesh Chatterjee^{1*}, Raj Gandhi^{1†}, Jyotsna Singh^{2‡},

¹*Harish-Chandra Research Institute, Chhatnag Road, Jhansi, Allahabad 211 019, India*

²*University of Lucknow, Lucknow 226007, India*

January 11, 2021

Abstract

We study the sensitivity of the Iron Calorimeter (ICAL) at the India-Based Neutrino Observatory (INO) to Lorentz and CPT violation in the neutrino sector. Its ability to identify the charge of muons in addition to their direction and energy makes ICAL a useful tool in putting constraints on these fundamental symmetries. Using resolution, efficiencies, errors and uncertainties obtained from ICAL detector simulations, we determine sensitivities to δb_{31} , which parametrizes the violations in the muon neutrino sector. We carry out calculations for three generic cases representing mixing in the CPT violating part of the hamiltonian, specifically, when the mixing is 1) small, 2) large, 3) the same as that in the PMNS matrix. We find that for both types of hierarchy, ICAL at INO should be sensitive to $\delta b_{31} \gtrsim 4 \times 10^{-23}$ GeV at 99 % C.L. for 500 kt-yr exposure, unless the mixing in the CPT violation sector is small.

1 Introduction

Invariance under the product of charge conjugation (C), parity (P) and time reversal (T), *i.e.* the CPT theorem [1–3], is a linchpin of present-day quantum field theories underlying particle physics. It is noteworthy that this invariance under the product of purely discrete symmetries is actually a consequence of the invariance of the Lagrangian (\mathcal{L}) under a connected continuous group, namely, proper Lorentz transformations. Additionally, it follows from the requirement that \mathcal{L} be hermitian and the interactions in the underlying field theory be local, with the fields obeying the commutation relations dictated by the spin-statistics theorem.

*email: animesh@hri.res.in

†email: raj@hri.res.in

‡email: jyo2210@yahoo.co.in

Theories attempting to unify gravity and quantum mechanics may, however, break such seemingly solid pillars of low energy effective field theories (like the Standard Model (SM)) via new physics associated with the Planck scale. For a general mechanism for the breaking of Lorentz symmetry in string theories, see, for instance, [4]. Other scenarios for such breaking have been discussed in [5] and [6]. Also, as shown in [7], a violation of CPT always breaks Lorentz invariance, while the converse is not true. A framework for incorporating CPT and Lorentz violation into a general relativistically extended version of the SM has been formulated in [8,9]. It is termed as the Standard Model Extension (SME), and our discussion in this paper will utilize the effective CPT violating (CPTV) terms that it introduces. Such terms, given the impressive agreement of the (CPT and Lorentz invariant) SM with all present day experiments, must of necessity be small.

A characteristic attribute of neutrino oscillations is the amplification, via interference, of the effects of certain small parameters (*e.g.* neutrino masses) in the underlying SM lagrangian. As discussed in [10] and [11], the CPT violation manifest in an effective SME hamiltonian can also be rendered measurable in neutrino oscillation experiments. Its non-observation, on the other hand, can be used to set impressive limits on CPT and Lorentz violation. This has been done, to cite a few recent examples, by IceCube [12], Double Chooz [13], LSND [14], MiniBooNE [15], MINOS [16] and Super Kamiokande [17]. Additionally, many authors have studied how best to parametrize and/or use neutrino oscillations and neutrino interactions to perform tests of CPT and Lorentz symmetry breaking in different contexts, ranging from neutrino factories and telescopes to long baseline, atmospheric, solar and reactor experiments, including those looking for supernova neutrinos [18–39].

In this article we study the sensitivity of a large atmospheric magnetized iron calorimeter to CPTV using a three flavour analysis with matter effects. As a reference detector for our study, we use the ICAL, the proposed detector for the India-Based Neutrino Observatory(INO) [40]. The main physics objective of ICAL is the determination of the neutrino mass hierarchy through the observation of earth matter effects in atmospheric neutrinos, as discussed, for instance, in [41–45]. However, its lepton charge identification capability renders it useful in measurements related to our purpose here.

In what follows, in Section 2 we review the perturbative phenomenological approach that allows us to introduce the effects of CPT violation in the neutrino oscillation probability, based on the SME. We examine effects at the probability level, in order to get a better understanding of the physics that drives the bounds we obtain using our event rate calculations. In section 3 we describe our method of analysis, and in section 4 we discuss our results, in the form the bounds on CPT violating terms. Section 5 summarizes our conclusions.

2 CPTV effects at the probability level

The effective Lagrangian for a single fermion field, with Lorentz violation [46] induced by new physics at higher energies can be written as

$$\mathcal{L} = i\bar{\psi}\partial_{\mu}\gamma^{\mu}\psi - m\bar{\psi}\psi - A_{\mu}\bar{\psi}\gamma^{\mu}\psi - B_{\mu}\bar{\psi}\gamma_5\gamma^{\mu}\psi , \quad (1)$$

where A_{μ} and B_{μ} are real numbers, hence A_{μ} and B_{μ} necessarily induce Lorentz violation, being invariant under boosts and rotations, for instance. Such violation under the group of proper

Lorentz transformations then leads to CPT violation [7]*.

The effective contribution to the neutrino Lagrangian can then be parametrized [18] as

$$\mathcal{L}_\nu^{CPTV} = \bar{\nu}_L^\alpha b_\mu^{\alpha\beta} \gamma^\mu \nu_L^\beta \quad (2)$$

where $b_\mu^{\alpha\beta}$ are four Hermitian 3×3 matrices corresponding to the four Dirac indices μ and α, β are flavor indices. Therefore the effective Hamiltonian in the vacuum for ultra-relativistic neutrinos with definite momentum p is

$$H \equiv \frac{MM^\dagger}{2p} + b_0 \quad (3)$$

where M is the neutrino mass matrix in the CPT conserving limit. As mentioned above, the b_μ parameterize the extent of CPT violation.

In many experimental situations, the neutrino passes through appreciable amounts of matter. Accounting for this, the Hamiltonian with CPT violation in the flavour basis [†] becomes

$$H_f = \frac{1}{2E} \cdot U_0 \cdot D(0, \Delta m_{21}^2, \Delta m_{31}^2) \cdot U_0^\dagger + U_b \cdot D_b(0, \delta b_{21}, \delta b_{31}) \cdot U_b^\dagger + D_m(V_e, 0, 0) \quad (4)$$

where U_0 & U_b are unitary matrices and $V_e = \sqrt{2}G_F N_e$, where G_F is the fermi coupling constant and N_e is the electron number density. Value of $V_e = 0.76 \times 10^{-4} \times Y_e [\frac{\rho}{g/cc}]$ eV, where Y_e is the fraction of electron, which is ≈ 0.5 for earth matter and ρ is matter density inside earth. D , D_m and D_b are diagonal matrices with their elements as listed. Here $\delta b_{i1} \equiv b_i - b_1$ for $i = 2, 3$, where b_1, b_2 and b_3 are the eigenvalues of b .

As is well-known, in standard neutrino oscillations, U_0 is parametrized by three mixing angles $(\theta_{12}, \theta_{23}, \theta_{13})$ and one phase δ_{CP} .[‡] Similarly (see footnote), any parametrization of the matrix U_b , needs three angles $(\theta_{b12}, \theta_{b23}, \theta_{b13})$ and six phases. Thus H_f contains six mixing angles $(\theta_{12}, \theta_{23}, \theta_{13}, \theta_{b12}, \theta_{b23}, \theta_{b13})$ and seven phases.

It is clear that the results will depend on the mixing angles in the CPT violation sector. In what follows, we examine the effects of three different representative sets of mixing angles, 1) small mixing $(\theta_{b12} = 6^\circ, \theta_{b23} = 9^\circ, \theta_{b13} = 3^\circ)$, 2) large mixing $(\theta_{b12} = 38^\circ, \theta_{b23} = 45^\circ, \theta_{b13} = 30^\circ)$ and the third set 3) uses the same values as the mixing in neutrino UPMNS, $(\theta_{b12} = \theta_{12}, \theta_{b23} = \theta_{23}, \theta_{b13} = \theta_{13})$. We use the recent best fit neutrino oscillation parameters in our calculation as mentioned in table 1.

*CPT violation may also occur if particle and anti-particle masses are different. Such violation, however, also breaks the locality assumption of quantum field theories [7]. We do not consider this mode of CPT breaking in our work.

[†]We note that the matrices appearing in the three terms in eq 3 can in principle be diagonal in different bases, one in which the neutrino mass matrix is diagonal, a second one in which the Lorentz and CPT violating interactions are diagonal, and a third flavour basis.

[‡]In general for an N dimensional unitary matrix, there are N independent rotation angles (i.e. real numbers) and $N(N+1)/2$ imaginary quantities (phases) which define it. For Dirac fields, $(2N-1)$ of these may be absorbed into the representative spinor, while for Majorana fields this can be done for N phases. In the latter case, the $N-1$ additional phases in U_0 become irrelevant when the product MM^\dagger is taken.

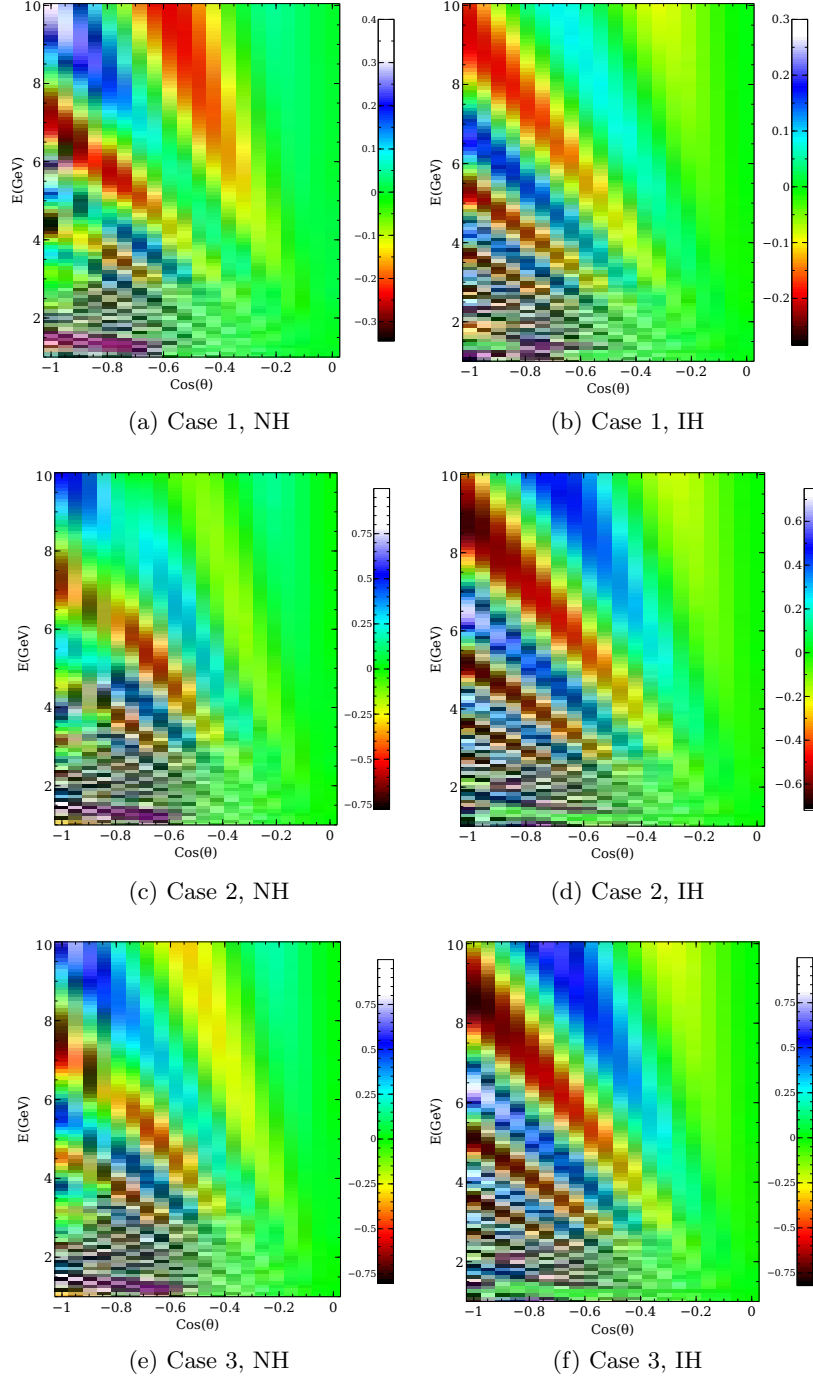


Figure 1: The oscillograms of $\Delta P = (P_{\nu_\mu \nu_\mu}^{U_b \neq 0} - P_{\nu_\mu \nu_\mu}^{U_b = 0})$ for 3 different mixing cases have been shown. The value of $\delta b_{31} = 3 \times 10^{-23} GeV$ is taken for $U_b \neq 0$. Left and right panels are for Normal and Inverted hierarchy respectively.

Before going into the detailed numerical calculations, we can roughly estimate the bound on CPTV term. As an example, let us assume case 3) *i.e* when $U_b = U_0$, then δb can effectively be added to $\frac{\Delta m^2}{2E}$. If we take 10 GeV for a typical neutrino energy, the value of $\frac{\Delta m^2}{2E}$ will be about 10^{-22} GeV. Assuming the CPT violating term to be of the same order, and assuming that neutrino mass splitting can be measured at ICAL to 10% accuracy, we expect sensitivity to δb values of approximately around 10^{-23} GeV.

From case 3 above, we note further that in its probability expressions, δb_{21} will always appear with the smaller (by a factor of 30) mass squared difference Δm_{21}^2 . Thus we expect its effects on oscillations will be subdominant in general, limiting the capability of atmospheric neutrinos to constrain it, and in our work we have not been able to put useful constraints on δb_{21} . Thus, our effort has been to find a method which will give the most stringent bounds on CPT violation as parametrized by δb_{31} . For simplicity, all phases are set to zero, hence the distinction between Dirac and Majorana neutrinos with regard to the number of non-trivial phases does not play a role in what follows. Moreover, in the approximation where the effects of δb_{21} are much smaller than those of δb_{31} , the impact of at least some of the nontrivial phases anyway will be negligible. We also study the effect and impact of hierarchy in putting constraints on CPTV violating terms.

We also note here previously obtained limits on the parameters of U_b . The solar and KamLAND data [19] gives the bound $\delta b \lesssim 1.6 \times 10^{-21}$ GeV. In [20] by studying the ratio of total atmospheric muon neutrino survival rates, (*i.e* two flavour approach different from the one in the present paper), it was shown that, for a 50 kt magnetized iron calorimeter, $\delta b \lesssim 3 \times 10^{-23}$ GeV should be attainable with a 400 kT-yr exposure. Using a two-flavor analysis, it was noted in [21] that a long baseline ($L = 735$ km) experiment with a high energy neutrino factory can constrain δb to $\lesssim 10^{-23}$ GeV. A formalism for a three flavour analysis was presented in [22] and bounds of the order of $\delta b \lesssim 3 \times 10^{-23}$ GeV were calculated for the upcoming NoVA experiment and for neutrino factories. It has also been shown in [25], that a bound of $\delta b_{31} \lesssim 6 \times 10^{-24}$ GeV at 99% CL can be obtained with a 1 Mt-yr magnetized iron detector. Global two-flavor analysis of the full atmospheric data and long baseline K2K data puts the bound $\delta b \lesssim 10^{-23}$ GeV [47].[§]

Prior to discussing the results of our numerical simulations, it is useful to examine these effects at the level of probabilities. We note that the matter target in our case is CP asymmetric, which will automatically lead to effects similar to those induced by \mathbf{U}_b . In order to separate effects arises due to dynamical CPT violation from those originating due to the CP asymmetry of the earth, it helps to consider the difference in the disappearance probabilities with \mathbf{U}_b effects turned on and off, respectively. We use the difference in probabilities

$$\Delta P = P_{\nu_\mu \nu_\mu}^{U_b \neq 0} - P_{\nu_\mu \nu_\mu}^{U_b = 0}. \quad (5)$$

We do this separately for ν_μ and $\bar{\nu}_\mu$ events with NH and IH assumed as the true hierarchy. The results are shown in the figures 1 – 2. (We note that at the event level, the total muon events receive contributions from both the $P_{\nu_\mu \nu_\mu}$ disappearance and $P_{\nu_e \nu_\mu}$ appearance channels, and the same is true for anti-neutrinos. In our final numerical results, we have taken both these

[§]Note that the bounds obtained in these papers, and the bounds that we will obtain below, are on the absolute value of δb , since in principle this quantity can be either positive or negative in the same way the Δm_{ij}^2 can be positive or negative. In our plots, where necessary, we assume it to be positive for simplicity.

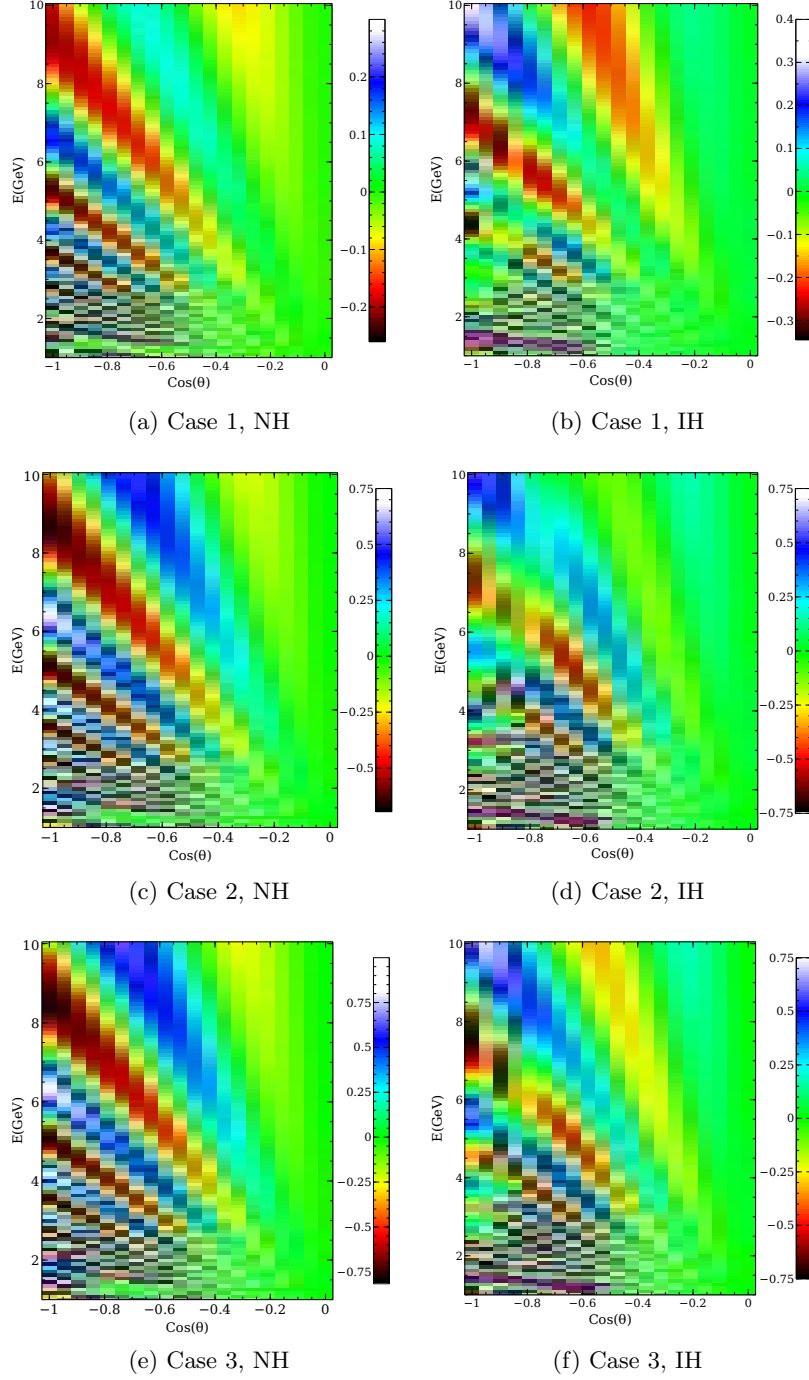


Figure 2: The oscillograms of $\Delta P = (P_{\bar{\nu}_\mu \nu_\mu}^{U_b \neq 0} - P_{\bar{\nu}_\mu \nu_\mu}^{U_b = 0})$ for 3 different mixing cases have been shown. The value of $\delta b_{31} = 3 \times 10^{-23} GeV$ is taken for $U_b \neq 0$. Left and right panels are for Normal and Inverted hierarchy respectively.

contributions into account).

Several general features are apparent in figures 1-2. First, effects are uniformly small at shorter baselines irrespective of the value of the energy. From the 2 flavour analysis, *e.g.* [20] we recall that the survival probability difference in vacuum is proportional to $\sin(\frac{\delta m^2 L}{2E}) \sin(\delta b L)$. The qualitative feature that CPT effects are larger at long baselines continues to be manifest even when one incorporates three flavour mixing and the presence of matter, and this is brought out in all the figures.

Secondly, as is well-known, matter effects are large and resonant for neutrinos and NH, and for anti-neutrinos with IH. Thus in both these cases, they mask the (smaller) effect of CPT stemming from U_b . Hence for neutrino events, CPT sensitivity is significantly higher if the hierarchy is inverted as opposed to normal, and the converse is true for anti-neutrino events. Finally, effects are largest for cases 3) and 2), and smaller for case 1). The effect is smaller for case 1) is due to the fact that mixing is very small compared to other two. The origin of the difference for the case 2) and 3) is likely due to the fact that CPT violating effects are smaller when θ_{b13} is large, as shown in fig 3.

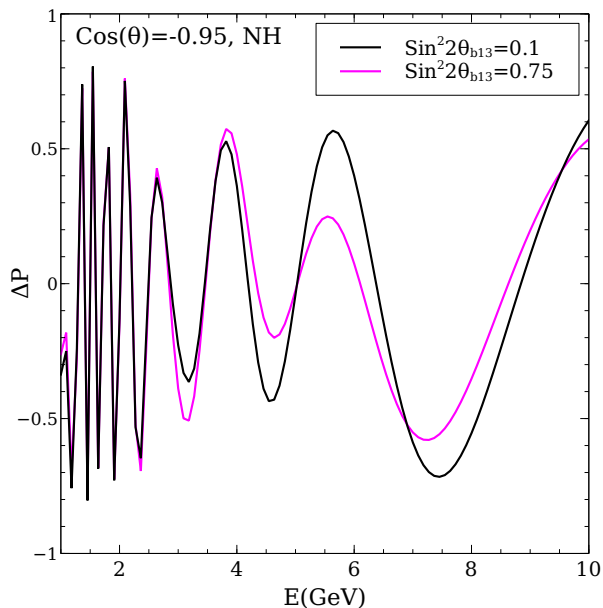


Figure 3: The difference of the $P_{\nu_\mu \nu_\mu}$ with and without CPTV for $\delta b_{31} = 3 \times 10^{-23} \text{GeV}$ for two θ_{b13} values as a function of energy for a specific value of zenith angle. All other oscillation parameters are same.

We carry through this mode of looking at the difference between the case when \mathbf{U}_b is non-zero and zero respectively to the event and χ^2 levels in our calculations below. To use the lepton charge identification capability of a magnetized iron calorimeter optimally, we calculate χ^2 from μ^- and μ^+ events separately. Following this procedure, the contribution arising through matter being CPT asymmetric will expectedly cancel for any given zenith angle and energy. The numerical procedure adopted and the details of our calculation are provided in the following section.

3 Numerical procedure

Our work uses the ICAL detector as a reference configuration, but the qualitative content of the results will hold for any similar detector. Magnetized iron calorimeters typically have very good energy and direction resolution for reconstructing μ^+ and μ^- events. The analysis proceeds in two steps: (1) Event simulation (2) Statistical procedure and the χ^2 analysis.

3.1 Event simulation

We use the NUANCE [48] neutrino generator to generate events. The ICAL detector composition and geometry are incorporated within NUANCE and atmospheric neutrino fluxes(Honda et al. [49]) have been used. In order to reduce the Monte Carlo (MC) fluctuations in the number of events given by NUANCE, we generate a very large number of neutrino events with an exposure of $50 \text{ kt} \times 1000 \text{ years}$ and then finally normalize to 500 kt-yr .

Each charged-current neutrino event is characterized by neutrino energy and neutrino zenith angle, as well as by a muon energy and muon zenith angle. In order to save on computational time, we use a re-weighting algorithm to generate oscillated events. This algorithm, takes the neutrino energy and angle for each event and calculates probabilities $P_{\nu_\mu\nu_\mu}$ and $P_{\nu_\mu\nu_e}$ for any given set of oscillation parameters. It then compares it with a random number r between 0 to 1. If $r < P_{\nu_\mu\nu_e}$, then it is classified as a ν_e event. If $r > (P_{\nu_\mu\nu_e} + P_{\nu_\mu\nu_\mu})$, it classified as a ν_τ event. If $P_{\nu_\mu\nu_e} \leq r \leq (P_{\nu_\mu\nu_e} + P_{\nu_\mu\nu_\mu})$, then it is considered to come from an atmospheric ν_μ which has survived as a ν_μ . Similarly muon neutrinos from the oscillation of ν_e to ν_μ are also calculated using this reweighting method.

Oscillated muon events are binned as a function of muon energy and muon zenith angle. We have divided each of the ten energy bins into 40 zenith angle bins. These binned data are folded with detector efficiencies and resolution functions as described in equation (6) to simulate reconstructed muon events. In this work we have used the (i) muon reconstruction efficiency (ii) muon charge identification efficiency (iii) muon energy resolution (iv) muon zenith angle resolution, obtained by the INO collaboration [50], separately for μ^+ and μ^- .

The measured muon events after implementing efficiencies and resolution are

$$N(\mu^-) = \int dE_\mu \int d\theta_\mu [R_{E_\mu} R_{\theta_\mu} (R_{eff} C_{eff} N_{osc}(\mu^-) + \bar{R}_{eff} (1 - \bar{C}_{eff}) N_{osc}(\mu^+))] \quad (6)$$

where $R_{eff}, C_{eff}, \bar{R}_{eff}, \bar{C}_{eff}$ are reconstruction and charge identification efficiencies for μ^- and μ^+ respectively, N_{osc} is the number of oscillated muons in each true muon energy and zenith angle bin and $R_{E_\mu}, R_{\theta_\mu}$ are energy and angular resolution functions.

The energy and angular resolution function in Gaussian form are given by

$$R_E = \frac{1}{\sqrt{2\pi}\sigma_E} \exp \left[-\frac{(E_m - E_t)^2}{2\sigma_E^2} \right] \quad (7)$$

$$R_\theta = N_\theta \exp \left[-\frac{(\theta_t - \theta_m)^2}{2(\sigma_\theta)^2} \right] \quad (8)$$

Here E_m , E_t and θ_m, θ_t are measured and true energy and angle respectively. N_θ is the normalization constant, σ_θ, σ_E are angular and energy smearing of muons. σ_θ, σ_E are obtained from ICAL simulations [50].

3.2 Statistical procedure and the χ^2 analysis

| Oscillation parameter | Best fit values | Oscillation parameter | Best fit values |
|--|----------------------|----------------------------------|----------------------------|
| $\sin^2 2\theta_{12}$ | 0.86 | δ_{CP} | 0.0 |
| $\sin^2 2\theta_{23}$ | 1.0 | $\sin^2 2\theta_{b12}$ | 1) 0.043, 2) 0.94, 3) 0.86 |
| $\sin^2 2\theta_{13}$ | 0.1 | $\sin^2 2\theta_{b23}$ | 1) 0.095, 2) 1.0, 3) 1.0 |
| Δm_{21}^2 (eV ²) | 7.5×10^{-5} | $\sin^2 2\theta_{b13}$ | 1) 0.011, 2) 0.75, 3) 0.1 |
| $ \Delta m_{32}^2 $ (eV ²) | 2.4×10^{-3} | $\delta_b, \phi_{b2}, \phi_{b3}$ | 0.0, 0.0, 0.0 |

Table 1: True values of the oscillation parameters used in the analysis

| Uncertainties | Values |
|-------------------------|--------|
| Flux Normalization | 20% |
| Tilt Factor | 5% |
| Zenith angle dependence | 5% |
| Overall cross section | 10% |
| Overall systematic | 5% |

Table 2: Systematic uncertainties used in the χ^2 analysis

We have generated event rate data with the true values of oscillation parameters given in Table 1 and assuming no CPT violation, these are defined as N^{ex} . They are then fitted with another set of data, labelled as (N^{th}), where we have assumed CPT violation. The statistical significance of the difference between these two sets of data will provide constraints on the CPT violation parameters.

We define χ^2 for the data as

$$\chi_{pull}^2 = \min_{\xi_k} [2(N^{th'} - N^{ex} - N^{ex} \ln(\frac{N^{th'}}{N^{ex}})) + \sum_{k=1}^{npull} \xi_k^2] \quad (9)$$

where

$$N^{th'} = N^{th} + \sum_{k=1}^{npull} c^k \xi_k \quad (10)$$

npull is the number of pull variable, in our analysis we have taken npull=5. ξ_k is the pull variable and c^k are the systematic uncertainties. We have used 5 systematic uncertainties in this analysis as mentioned in Table 2 as generally used in the other analysis of the collaboration. We have assumed a Poissonian distribution for χ^2 because for higher energy bins the number of

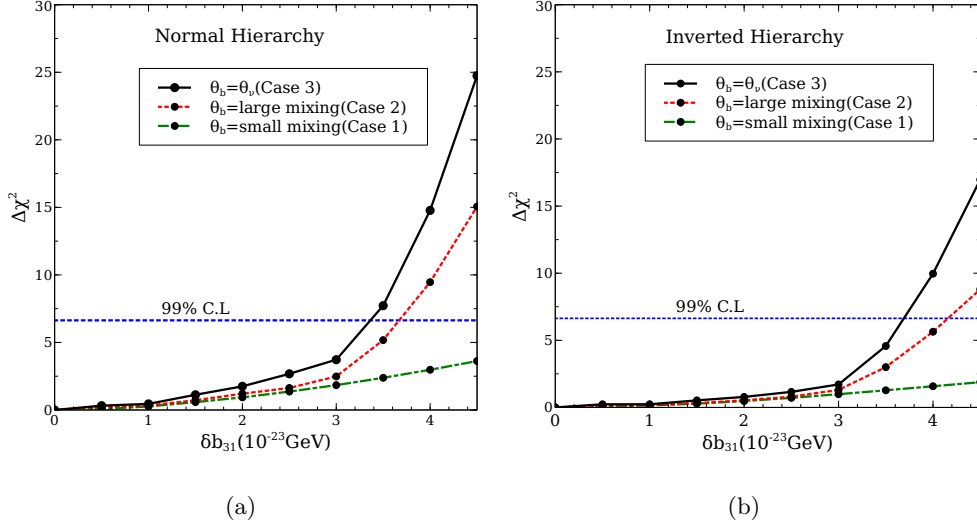


Figure 4: $\Delta\chi^2$ as a function of δb_{31} for different mixing of θ_b . Best fit oscillation parameters used as mentioned in table 1. The results are marginalized over θ_{23} , θ_{13} , δ_{CP} , Δm_{31}^2 and δb_{21} . Left and right panel are for Normal and Inverted hierarchy respectively.

atmospheric events will be small.

Since ICAL can discriminate charge of the particle, it is useful to calculate $\chi^2(\mu^-)$ and $\chi^2(\mu^+)$ separately for μ^- and μ^+ events and then added to get total χ^2 . We have marginalized the total χ^2 within a 3σ range of the best fit value. χ^2 has been marginalized over the oscillation parameters Δm_{31}^2 , θ_{23} , θ_{13} , δ_{CP} , δb_{21} for both normal and inverted hierarchy with μ^+ and μ^- separately for given set of input data.

4 Results

Figure(4) illustrates $\Delta\chi^2$ analysis performed by marginalizing over all the oscillation parameters Δm_{31}^2 , θ_{23} , θ_{13} within a 3σ range of their best fit values as given in Table 1. δ_{CP} is marginalized over 0 to 2π . δb_{21} is marginalized over the range 0 to 5×10^{-23} GeV. Left and right panel are for the Normal and Inverted Hierarchy respectively. While from figure(4) we see that the best bounds arise for case 3) for both the hierarchy, where mixing in the CPTV sector is the same as in the case of neutrino mixing, good bounds are also obtainable for large mixing. Since θ_{b12} and θ_{b23} in both cases 2) and 3) are large, the origin of this difference is likely due to the fact that CPT violating effects are smaller when θ_{b13} is large, as shown in fig 3.

From figure(4) we see that 99% C.L. or better constraints on the CPT violating parameter, δb_{31} are possible for both hierarchies if it is $\gtrsim 4 \times 10^{-23}$ GeV, if the mixing in the CPTV sector is not small.

It is clear from the fig 5 that if marginalization over the hierarchy is carried out, the con-

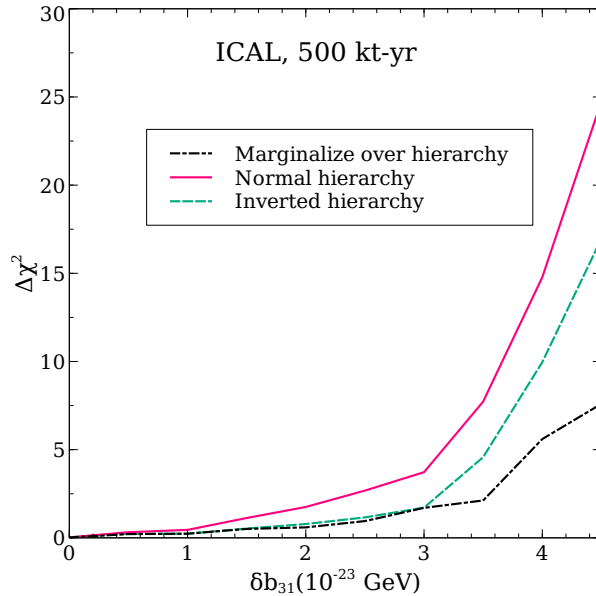


Figure 5: $\Delta\chi^2$ as a function of δb_{31} for case 3) is shown. The Red curve represents that both sets of data has Normal hierarchy as true hierarchy, and the green curve for Inverted hierarchy respectively. Black curve shows the bounds where hierarchy is marginalized over.

straints are considerably weaker. Hence a knowledge of the hierarchy certainly helps in getting useful constraints on CPT. The sensitivities obtained are comparable to those anticipated from other types of experiments and estimates in the literature [19–22, 25].

5 Conclusions:

A magnetized iron calorimeter like ICAL, with its attributes of good energy and angular resolution for muons and its charge identification capability can be a useful tool in investigating Lorentz and CPT violation stemming from physics at higher energy scales, even though its main physics objective may be hierarchy determination. Using resolutions, efficiencies, errors and uncertainties generated by ICAL detector simulation, we have calculated reliable sensitivities to the presence of CPTV in such a detector.

It is, of course, clear that the exact value of the constraint on CPT violation depends on the choice of mixing angles in U_b . We have carried out our calculations for three representative cases, those for which the mixing is 1) small, 2) large and 3) similar to the PMNS mixing. We find that for both types of hierarchy, ICAL should be sensitive to $\delta b_{31} \gtrsim 4 \times 10^{-23}$ GeV at 99% C.L. with 500 kt-yr of exposure, unless the mixing in the CPTV sector is small. As discussed earlier, CP (and CPT) effects due to earth matter asymmetry are subtracted out.

Our study pertains to the type of CPTV that may be parametrized by Equation 1, which stems from explicit Lorentz violation, and to the muon detection channel. We have not considered the CPTV that arises from differing masses for particles and anti-particles. Finally, we note

that in order to obtain good sensitivity to CPTV, knowing the hierarchy will be an important asset, which will anyway be done in a detector like ICAL.

6 Acknowledgments

We thank the INO physics and simulation group for their help. We also especially thank Amitava Raychaudhuri, Amol Dighe, M. V. N. Murthy and S Uma Sankar for the useful discussions and comments. A.C thanks Pomita Ghoshal and Anushree Ghosh for the help during the work.

References

- [1] W.Pauli, "Exclusion principle, Lorentz group and reflection of space-time and charge", London, Pergamon Press, 1955
- [2] G.Grawert et al., Fortschr. Phys.7 291 (1959).
- [3] For a review and a comprehensive and historical list of references on the CPT theorem, see I. S. Tsukerman, arXiv:1006.4989 [hep-ph].
- [4] V. A. Kostelecky and S. Samuel, Phys. Rev. D **39**, 683 (1989).
- [5] G. Amelino-Camelia et al. , Nature, **393**, 763 (1998); D.Sudarsky et al., Phys. Rev. D **68**, 024010 (2003); J. Alfaro et al., Phys. Rev. Lett. **84**, 2318 (2000).
- [6] M. R. Douglas and N. A. Nekrasov, Rev. Mod. Phys. **73**, 977 (2001) [hep-th/0106048].
- [7] O. W. Greenberg, Phys. Rev. Lett. **89**, 231602 (2002) [hep-ph/0201258].
- [8] D. Colladay and V. A. Kostelecky, Phys. Rev. D **58**, 116002 (1998) [hep-ph/9809521].
- [9] V. A. Kostelecky, Phys. Rev. D **69**, 105009 (2004) [hep-th/0312310].
- [10] V. A. Kostelecky and M. Mewes, Phys. Rev. D **70**, 031902 (2004) [hep-ph/0308300].
- [11] V. A. Kostelecky and M. Mewes, Phys. Rev. D **69**, 016005 (2004) [hep-ph/0309025].
- [12] R. Abbasi *et al.* [IceCube Collaboration], Phys. Rev. D **82**, 112003 (2010) [arXiv:1010.4096 [astro-ph.HE]].
- [13] Y. Abe *et al.* [Double Chooz Collaboration], Phys. Rev. D **86**, 112009 (2012) [arXiv:1209.5810 [hep-ex]].
- [14] L. B. Auerbach *et al.* [LSND Collaboration], Phys. Rev. D **72**, 076004 (2005) [hep-ex/0506067].
- [15] A. A. Aguilar-Arevalo *et al.* [MiniBooNE Collaboration], Phys. Lett. B **718**, 1303 (2013) [arXiv:1109.3480 [hep-ex]].
- [16] P. Adamson *et al.* [MINOS Collaboration], Phys. Rev. D **85**, 031101 (2012) [arXiv:1201.2631 [hep-ex]].

- [17] T. Akiri, arXiv:1308.2210 [hep-ph].
- [18] S. R. Coleman and S. L. Glashow, Phys. Rev. D **59**, 116008 (1999) [hep-ph/9812418].
- [19] J. N. Bahcall, V. Barger and D. Marfatia, Phys. Lett. B **534**, 120 (2002) [hep-ph/0201211].
- [20] A. Datta, R. Gandhi, P. Mehta and S. U. Sankar, Phys. Lett. B **597**, 356 (2004) [hep-ph/0312027].
- [21] V. D. Barger, S. Pakvasa, T. J. Weiler and K. Whisnant, Phys. Rev. Lett. **85**, 5055 (2000) [hep-ph/0005197].
- [22] A. Dighe and S. Ray, Phys. Rev. D **78**, 036002 (2008) [arXiv:0802.0121 [hep-ph]].
- [23] J. S. Diaz, V. A. Kostelecky and M. Mewes, Phys. Rev. D **80**, 076007 (2009) [arXiv:0908.1401 [hep-ph]].
- [24] J. S. Diaz, arXiv:0909.5360 [hep-ph].
- [25] A. Samanta, Phys. Lett. B **693**, 296 (2010) [arXiv:1005.4851 [hep-ph]].
- [26] N. Engelhardt, A. E. Nelson and J. R. Walsh, Phys. Rev. D **81**, 113001 (2010) [arXiv:1002.4452 [hep-ph]].
- [27] S. T. Scully and F. W. Stecker, Astropart. Phys. **34**, 575 (2011) [arXiv:1008.4034 [astro-ph.CO]].
- [28] J. Ellis, H. -T. Janka, N. E. Mavromatos, A. S. Sakharov and E. K. G. Sarkisyan, Phys. Rev. D **85**, 045032 (2012) [arXiv:1110.4848 [hep-ph]].
- [29] Koranga, Bipin Singh and Kumar, Vinod and Jha, A., Int. J. Theor. Phys. **50** (2011), 2609-2613.
- [30] V. A. Mitsou, J. Phys. Conf. Ser. **335**, 012003 (2011) [arXiv:1104.1149 [hep-ph]].
- [31] I. Motie and S. -S. Xue, Int. J. Mod. Phys. A **27**, 1250104 (2012) [arXiv:1206.0709 [hep-ph]].
- [32] P. W. Gorham, A. Connolly, P. Allison, J. J. Beatty, K. Belov, D. Z. Besson, W. R. Binns and P. Chen *et al.*, Phys. Rev. D **86**, 103006 (2012) [arXiv:1207.6425 [astro-ph.HE]].
- [33] S. Chakraborty, A. Mirizzi and G. Sigl, Phys. Rev. D **87**, 017302 (2013) [arXiv:1211.7069 [hep-ph]].
- [34] T. Katori [LSND and MiniBooNE and Double Chooz Collaborations], PoS ICHEP **2012**, 008 (2013) [arXiv:1211.7129 [hep-ph]].
- [35] B. Altschul, Phys. Rev. D **87**, 096004 (2013) [arXiv:1302.2598 [hep-ph]].
- [36] Z. -K. Guo and J. -W. Hu, Phys. Rev. D **87**, 123519 (2013) [arXiv:1303.2813 [astro-ph.CO]].
- [37] E. Borriello, S. Chakraborty, A. Mirizzi and P. D. Serpico, Phys. Rev. D **87**, 116009 (2013) [arXiv:1303.5843 [astro-ph.HE]].

- [38] J. S. Diaz, arXiv:1307.6845.
- [39] F. Rossi-Torres, arXiv:1307.0884 [hep-ph].
- [40] M. S. Athar et al. [INO Collaboration], INO-2006-01
- [41] D. Indumathi and M. V. N. Murthy, Phys. Rev. D **71**, 013001 (2005) [hep-ph/0407336].
- [42] R. Gandhi, P. Ghoshal, S. Goswami, P. Mehta, S. U. Sankar and S. Shalgar, Phys. Rev. D **76**, 073012 (2007) [arXiv:0707.1723 [hep-ph]].
- [43] A. Samanta, Phys. Rev. D **81**, 037302 (2010) [arXiv:0907.3540 [hep-ph]].
- [44] M. Blennow and T. Schwetz, JHEP **1208**, 058 (2012) [Erratum-ibid. **1211**, 098 (2012)] [arXiv:1203.3388 [hep-ph]].
- [45] A. Ghosh, T. Thakore and S. Choubey, JHEP **1304**, 009 (2013) [arXiv:1212.1305].
- [46] D. Colladay and V. A. Kostelecky, Phys. Rev. D **55**, 6760 (1997) [hep-ph/9703464].
- [47] M. C. Gonzalez-Garcia and M. Maltoni, Phys. Rev. D **70**, 033010 (2004) [hep-ph/0404085].
- [48] D. Casper, Nucl. Phys. Proc. Suppl. **112**, 161 (2002) [hep-ph/0208030].
- [49] M. Honda, T. Kajita, K. Kasahara and S. Midorikawa, Phys. Rev. D **83**, 123001 (2011) [arXiv:1102.2688 [astro-ph.HE]].
- [50] “A Simulations Study of the Response of ICAL Detector to Muons”, A. Chatterjee, Meghna K. K., K. Rawat, T. Thakore et al., INO Collaboration.